A&A 390, L5–L9 (2002)
DOI: 10.1051/0004-6361:20020890


Astronomy & Astrophysics



# A twisted jet from R Mon⋆

T. A. Movsessian[1], T. Yu. Magakian[1], and V. L. Afanasiev[2]

[1] Byurakan Astrophysical Observatory, Aragatsotn prov., 378433 Armenia
and Isaac Newton Institute of Chile, Armenian Branch
e-mail: tigmag@sci.am
[2] Special Astrophysical Observatory, N.Arkhyz, Karachaevo-Cherkesia, 369167, Russia
e-mail: vafan@sao.ru

Received 2 April 2002 / Accepted 11 June 2002

**Abstract.** We present the results of long-slit and integral-field spectroscopy of the R Mon Herbig-Haro jet. The data were obtained with the 6 m telescope. A slightly curved jet of 16″ in length is evident in [S II] lines. Maps of radial velocities and electron densities are shown. The difference between radial velocities on the sides of the jet as well as the density distribution can be considered as an indication of presence of the helical shock structure in the jet. This structure, having a DNA-like appearance, abruptly changes direction near the edges, which could account for the observed velocity variations. Radial velocities were determined also for the several knots in the HH 39 group. The kinematics of the system as a whole also suggests the precession of the outflow.

**Key words.** ISM: individual objects: R Mon – jets and outflows – kinematics and dynamics

## 1. Introduction

R Mon, associated with NGC 2261, the prototype cometary nebula (CN), is one of the best studied pre-main-sequence objects. First of all, R Mon is one of the brightest and best studied Herbig Ae/Be stars (Thé et al. 1994). NGC 2261 is one of the largest CN on the sky, with high surface brightness, though the distance of the object is significant – 750–800 pc (Close et al. 1997). On the other hand, in this object interesting manifestations of anisotropic activity of YSOs were discovered. Actually the R Mon – NGC 2261 system is one of the first objects where the existence of directed outflow was predicted and then discovered.

The interesting effect of the progressive blueshift of reflected absorption lines in the spectrum of NGC 2261 with increasing distance from R Mon (Stockton et al. 1975; Greenstein et al. 1976) was interpreted as evidence of possible anisotropic outflow from R Mon (Greenstein et al. 1979). Further evidence appeared when flattened molecular envelope and bipolar CO outflow in the northern (blueshifted) and southern (redshifted) directions were discovered by Canto et al. (1981). Yet more evidence emerged when Jones & Herbig (1982) found that the knots in HH 39 – a Herbig-Haro object lying on the axis of NGC 2261 7.5′ north of R Mon (Herbig 1968) – are moving directly away from R Mon. In the same paper they suggested that all these phenomena can be explained by the existence of a strong stellar wind, which is already anisotropic on the dimensions of the expanding envelope.

After that it was not too unexpected when a high velocity collimated jet in the direction of the axis of the nebula was discovered spectroscopically (Brugel et al. 1984). However, within 17 years after this discovery there has been no imaging of the jet of R Mon, because even with narrow band imagery it is virtually impossible to detect the jet against the bright background of the reflection nebula. Nor have any additional spectra of the jet been published since.

Among other important results one should note the discovery of the IR companion of R Mon at a distance of 0.7″ and of the interesting structures with helical filaments inside the nebula, seen with the aid of high resolution adaptive optics near-IR imagery and polarimetry (Close et al. 1997). This again increased the interest in this system.

In this paper we present the results of new long-slit and integral field spectroscopy of the R Mon system. Preliminary data of long-slit observations were published before (Magakian & Movsessian 1997).

## 2. Observations and data reduction

All observational data, presented here, were obtained with the 6 m telescope of the Special Astrophysical Observatory (Russia).

*Send offprint requests to*: T. A. Movsessian,
e-mail: tigmov@bao.sci.am

⋆ Based on observations collected with the 6 m telescope of the Special Astrophysical Observatory (SAO) of the Russian Academy of Sciences (RAS) which is operated under the financial support of Science Department of Russia (registration number 01-43).

Long-slit spectroscopy was performed with a prime focus long-slit spectrograph and 580 × 530 CCD on 1995 November 27. The spectral resolution was about 1.5 Å, the spatial resolution was about 0.4″/row. One group of spectra was obtained with the slit, oriented through R Mon in the probable direction of the outflow (PA = 350°), defined by the location of HH 39 group. Several spectra were taken also with the slit perpendicular to this direction (PA = 260°) and placed to 12″ to north from R Mon. Besides, we observed several brightest knots in HH 39, orienting the slit through the knots A, E, D, G. The data were reduced in MIDAS system. After standard reductions the row-by-row fitting and subtraction of continuum was performed to increase the detectability of emission lines.

We made several attempts to obtain the image of the jet with the aid of the various systems for integral-field spectroscopy, starting from 1995 February. The most successful results were obtained on 1999 November 11 with the MPFS (Multi-Pupil Fiber Spectrograph, see e.g. Afanasiev & Sil'chenko 2000). It is installed at the prime focus of the 6 m telescope. In this instrument, contrary to the classical TIGER systems (Bacon et al. 1995), fibers are used to rearrange micro-pupils on a pseudo-slit. 240 fibers transmit light from 15 × 16 square elements with size of 1″×1″ of the sky and the sky background is obtained in 4.5′ off the object (15 fibers). This new design provides a larger common spectral range. All the 255 spectra simultaneously are projected onto a 1034 × 1034 CCD. Our observations were performed in red spectral range (5650–7000 Å), with total exposure time 60 min (3 × 20 min) and the spectral resolution of 3 Å. Seeing was about 1.5″. During the observations we placed the micro-lens array in such a way that the main axis of the NGC 2261 nebula was directed through the diagonal of the matrix, and the star was kept just out of the matrix' corner.

The reduction of these data was done with the use of the specially developed by one of the authors (V.L.A.) package of IDL procedures, which includes bias-subtracting, flat-fielding, one-dimensional spectra extracting and building of 3D data cubes for further wavelength calibration and analysis. The one-element spectral characteristics, such as the fluxes in emission lines or continuum, velocities, densities etc., could then be arranged into two-dimensional arrays, mapping the observed part of the object. By the night sky lines we have estimated the accuracy of our velocity measurements as ±25 km s$^{-1}$.

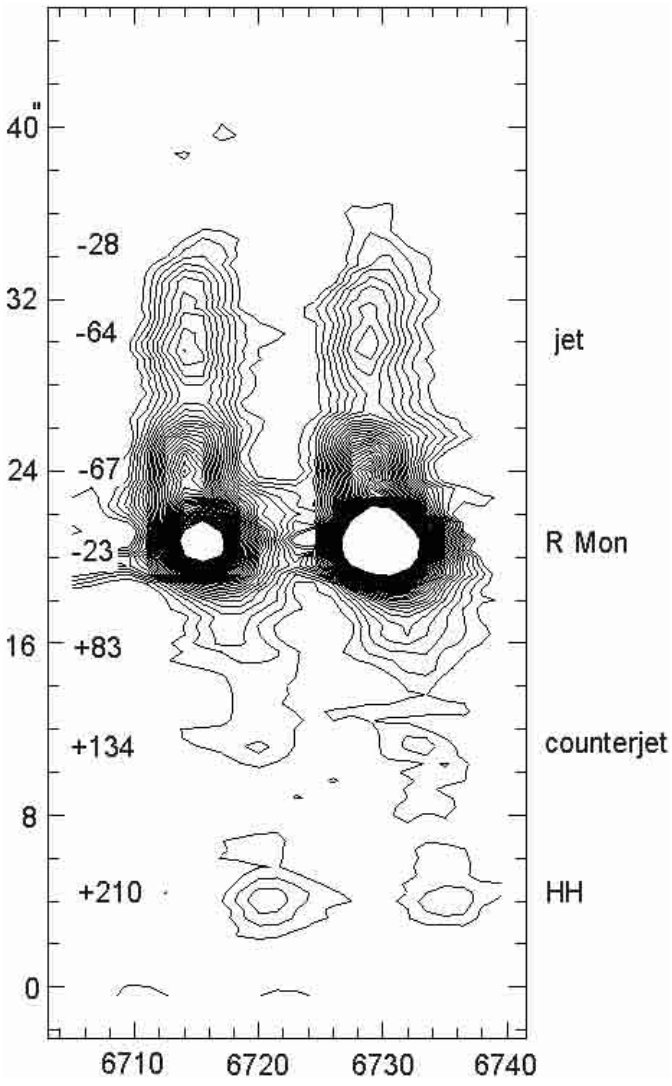


**Fig. 1.** The R Mon jet seen in [S II] lines on the long-slit spectrum. Stellar continuum and background emissions are subtracted. Abscissae units are in angströms, ordinates in arcsec. North is up. In the left side the heliocentric radial velocities for various parts of the jet are given.

## 3. Results

### 3.1. Long-slit observations

The spectrum of R Mon, according to our data, is nearly the same as described in the previous works, where observations made 20–30 years ago are presented. In the red spectral range one can see the very strong H$\alpha$ emission with superposed blueshifted absorption component, as well as the prominent emission lines of [S II], [O I] and Fe II. The radial velocity of the star, measured by the four brightest red Fe II lines, is +44 ± 8 km s$^{-1}$. This very well agrees with the measurments in the paper of Greenstein et al. (1976), where a value of +48 ± 9 km s$^{-1}$ was obtained in nearly the same way. Here it should be noted that we again didn't found perceptible difference between radial velocities of Fe II lines in the star and the nebula, although Stockton et al. (1975) found +27 ± 2 km s$^{-1}$ for the R Mon emission lines and, consequently, claim the existence of a +30 km s$^{-1}$ displacement of the nebular lines with respect to R Mon. Thus, the question arises which value can be assigned to systemic velocity. For the simplicity we shall further assume for this quantity +26 km s$^{-1}$, i.e. the velocity of CO cloud (see Jones & Herbig 1982).

The R Mon jet is best seen in [S II] lines, though its existence can be noted also in [O I] emission. Subtraction of the stellar continuum allows the study of its innermost parts very close to R Mon. As can be seen in Fig. 1, both the jet and counterjet start from the vicinity of R Mon and can be traced up to 14″ to the north and 18″ to the south. Jet as a whole has a clumpy appearance. The southern end of the counterjet comprises a very small (2″) knot, which could be considered as a HH object or a working surface of the counterjet. The main jet

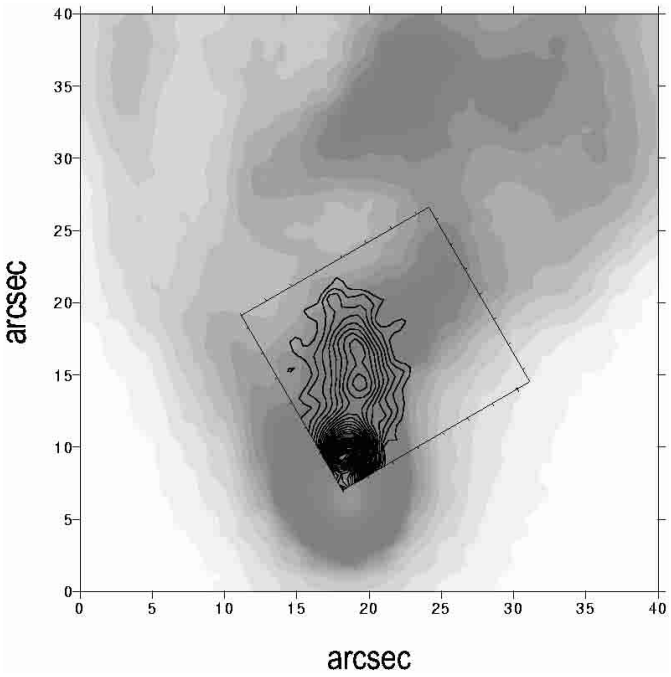


**Fig. 2.** Restored image of the jet in [SII]6716+6731 lines within the region covered by the micro-lens array, superposed on a grey scale *R* band image of NGC 2261 obtained with the 2.6 m telescope.

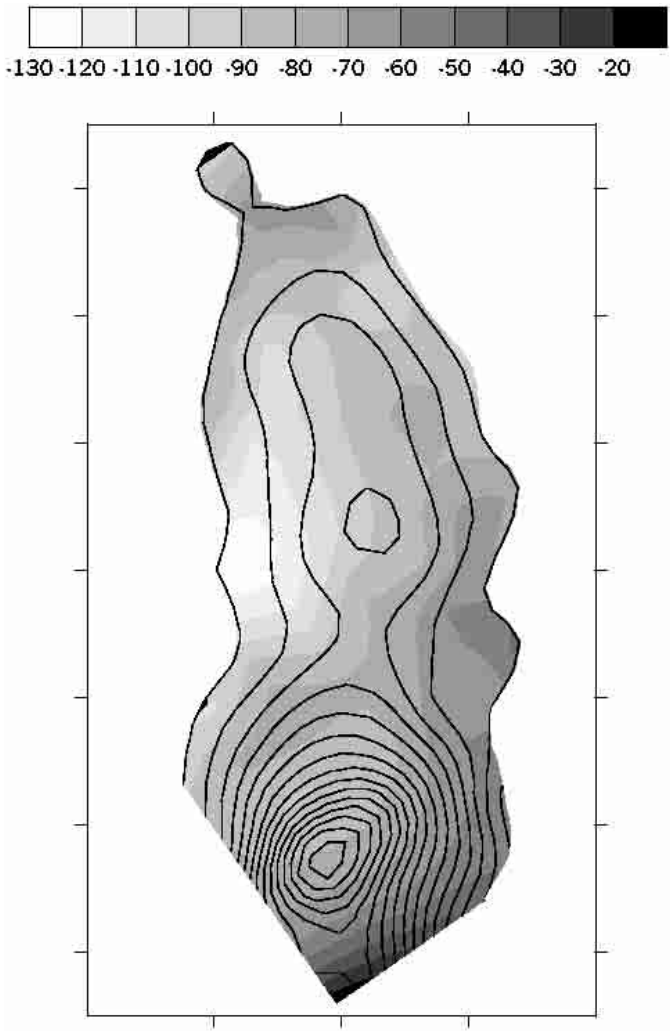


**Fig. 3.** Radial velocities field in the jet of R Mon, measured by [SII] lines. The shape of the jet is shown by isophotes. Scale marks in both axes correspond to 2″.

to the north is much brighter. Its brightness remains nearly constant up to the 5″ to north from R Mon. After that point (which corresponds to offset 26″ in Fig. 1) the intensity of the northern jet drops abruptly. It is interesting that this change occurs just on the northern boundary of the nebulous triangle near R Mon (Herbig 1968).

The electron density, derived from the ratio of [S II] lines, is rather high for the star (at least 2800 cm$^{-3}$). In the northern part of the jet, nearest to the star, it is about 960 cm$^{-3}$, and sharply drops to only 470 cm$^{-3}$ after the 5″ distance. Along the counterjet the electron density decreases in the typical for stellar jets fashion (see, e.g., Bacciotti & Eislöffel 1999) from 1240 cm$^{-3}$ just to the south from the star to 330 cm$^{-3}$ in the HH knot at the end. Of course, these values are only rough estimates due to the weakness of [S II] lines in the counterjet.

We measured also the radial velocity of [S II] lines. In the star they are definitely blueshifted (−23 km s$^{-1}$). The northern jet does not show the major changes in radial velocity. The velocity remains about −65 km s$^{-1}$ through nearly all length of the jet and probably becomes lower (in absolute sence: −28 km s$^{-1}$) near its end. This should be compared with the progressive increase (again in absolute sence) of the radial velocity along the counterjet (from +83 km s$^{-1}$ just to the south of the star to +210 km s$^{-1}$ in the small HH knot; see Fig. 1).

The FWHM width of the jet, estimated from the data, obtained with the slit perpendicular to the outflow, is about 2.5–3″ at 12″ to north of the star, but this, of course, is only the upper limit. The values of radial velocity and electron density perfectly correspond to the those measured at a distance of 12″, obtained from the data taken with the slit aligned along the jet axis.

On the whole, these values are in very good agreement with the previous estimates of Brugel et al. (1984). Of course, the latest observational techniques allowed to reveal many interesting details in the structure of the jet and its physical parameters.

### 3.2. MPFS observations

MPFS data are in good accordance with the long-slit observations and provide much more additional information about the spatial distribution of physical parameters. From the integral field spectroscopy we may construct an image of the jet in [SII] after accurate subtraction of the continuum.

In Fig. 2 the restored image of the jet in [S II] $\lambda$6716+$\lambda$6731 lines within the region, covered by the microlens array, is shown superposed on the *R* band image of the object, obtained with 2.6 m telescope of Byurakan observatory. The jet is seen very well and can be traced along the axis of NGC 2261 up to 16″ from the source. It is detected also in [O I] lines, though it is not so prominent (this image is not shown here). Its knotty morphology is obvious, the most interesting feature being the

**Table 1.** Heliocentric radial velocities of the HH 39 knots (in km $s^{-1}$).

| Object | $V_r$ |
|---|---|
| A | +65 ± 14 |
| E (north) | +30 ± 6 |
| E (south) | +6 ± 13 |
| D | +28 ± 12 |
| G | +48 ± 6 |

slightly curved shape of the jet. Comparing the dimensions of the jet and other parameters, estimated from the slit spectra, we must take into account that the slit observations were performed with the position angle 350°; meanwhile, as we see from Fig. 2, the jet as a whole is oriented in north-south direction.

We used [S II] lines to obtain the velocity field of the jet, which is presented in Fig. 3. These data are in good accordance with the results of long-slit spectroscopy (see Fig. 1). Here is ought to remind that star itself was outside the MPFS field. The mean velocity along the jet is about −80 km $s^{-1}$ without any perceptible gradient. But the most striking feature is the clear difference between the radial velocities on the eastern and western sides of the jet. This difference reaches up to 70 km $s^{-1}$.

Using the $\lambda$6716/$\lambda$6731 [S II] lines ratios, determined by all of the individual spectra, we also constructed the map of electron density in the jet, shown in Fig. 4. In this map several very interesting features are obvious.

Comparing it with the data of slit spectroscopy, we can see that this map confirms the steep decrease of the electron density in 5–6″ distance to north of R Mon. Besides, near the end of the jet a sharp density peak can be readily seen. This picture is rather common for the zones where collimated jet collides with ambient medium. It had been predicted theoretically (Raga 1986) and observationally found in many cases (e.g. Reipurth & Heathcote 1991; Magakian & Movsessian 1995). Also, the increase in density towards both sides of the jet should be noted. From Fig. 4 we see that these side zones of higher density have appearance of a non-continuous wall, surrounding a central cavity. They even show the traces of periodic structure. Moreover, this periodic structure is in good accordance with the low-level brightness isophotes of the jet in the sence that the clumps lie around the faint, outer edges of the jet.

### 3.3. HH 39

Spectral observations of the HH 39 Herbig-Haro object are rare (Jones & Herbig 1982; Walsh & Malin 1985). Our main aim was to obtain the radial velocity of the knots in HH 39, which is poorly known. In our slit spectrogramme it was possible to discern several emission condensations, which can be identified with the knots A, E, D, G (designations that of Walsh & Malin 1985), though one cannot be certain that the slit was passing through their centers.

All knots have the similar spectra of middle-excitation HH objects. Their radial velocities (presented in the Table 1) all are

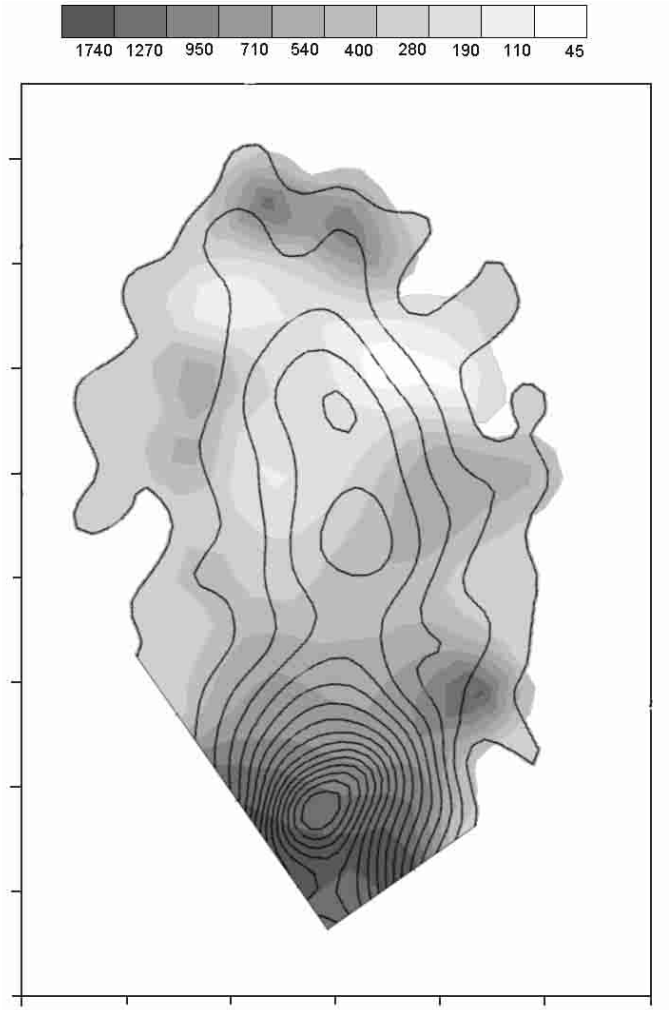


**Fig. 4.** Distribution of the electronic density in the jet of R Mon. Values are given in $cm^{-3}$. The shape of the jet is shown by isophotes. Scale marks in both axes correspond to 2″.

positive, in accordance with previous data. To determine these values we used the lines of [S II] red doublet and $\lambda$6583 [N II], as the least blended with the background emission. The HH 39E knot has obvious velocity gradient in S–N direction (see Table 1); similar gradient probably exists also in the knot A. Electron density in the knots varies from 850 $cm^{-3}$ in the knot A to 200 $cm^{-3}$ in the knot G.

## 4. Discussion and conclusion

As we see from our observations of R Mon with integral field spectrograph, the jet is considerably wide, with knotty structure and some periodic variations of intensity seen in lower isophotes. It is definitely curved relative to the line connecting the star and the HH 39 group. The most probable explanation of it can be the precession of the jet.

On the other hand, the velocity field creates an appearance of rotation of the jet. Indeed, rotation is the most obvious interpretation of the observed difference between the radial velocities on both sides of the jet. To our knowledge the only other example of the rotating stellar jet found so far is HH 212

(Davis et al. 2000; see also Wiseman et al. 2001). In that case, however, the rotation speed is lower by an order of magnitude.

We estimated the period of rotation using the following purely kinematic assumptions: width of the jet = 2.5″, distance = 760 pc (Close et al. 1997), linear speed of the rotation = 35 km $s^{-1}$. Simple calculations give about 800 years for the rotation period. To compare, the kinematic time for the jet is about 200 years (assuming 300 km $s^{-1}$ for the outflow velocity).

Such fast rotation could not be explained by simple rotation of the whole moving flow as solid body, because centrifugal force would disrupt it. We suggest a scenario with DNA-like helical shock filament weaved around the high-velocity outflow. This generates strong variations in the radial velocity near the edges, where the filament changes direction. In other words, we see shocked emission regions where the helical jet impacts the sides of the cavity seen in the $N_e$ density map. If viewed from the north along the jet axis, the jet would be seen to precess in an anti-clockwise direction. In the framework of this scenario the periodic variations of intensity and electron density can be explained as a spatially unresolved helical pattern of the shocks.

The interesting question arises as to the inclination of the jet and of the NGC 2261 cone as a whole. Jones & Herbig (1982) argue that the axis of the nebular cone lies nearly in the plane of the sky. Another set of arguments leads to the value $20 \pm 10°$ (Close et al. 1997) for the inclination of the jet. We can make yet another estimate for the jet inclination. Assuming the aforementioned values for the velocity of the outflow and for the systemic velocity, as well as $-70$ km $s^{-1}$ and $+80$ km $s^{-1}$ for the mean radial velocities of the jet and counterjet in the immediate vicinity of R Mon, one can easily obtain the inclination of 19° for the northern jet and 10° for the southern counterjet. As we see, these values are very close to those cited above. However, one should keep in mind that inclination of the nebular cone and that of the jet could differ for the certain moment of time due to the precession of the star's axis and/or of the plane of the orbit of the R Mon companion. The idea of the precessing jet is corroborated by the circumstance that the values of radial velocity of the knots in HH 39 are nearly equal to systemic velocity or even are more positive, though the northern jet near the star has negative radial velocity.

Formation of a helical shock structure around the axis of flows was predicted by MHD models of jets from young stellar objects (e.g. Shibata & Kudoh 1999). In various cases, depending on the flow velocity and ambient density, the manifestations of helical structures could be different, producing both the dusty spiral structures, observed in reflected light in several cometary nebulae (Movsessian & Magakian 1999; Close et al. 1997), as well as in shocked emission, as in the case of L1551 IRS5 jet (Itoh et al. 1999).

We can conclude that R Mon jet is well worth studying with higher spatial resolution.

*Acknowledgements.* We thank E.R. Hovhannessian for the reduction of the HH 39 spectra. We are grateful to Dr. M. D. Smith and to the referee Dr. C. J. Davis for many helpful comments and suggestions. This work was partially supported by INTAS grant 00-00287 and ANSEF grant No. PS103-01.

## References

Afanasiev, V. L., & Sil'chenko, O. K. 2000, AJ, 119, 126
Bacciotti, F., & Eislöffel, J. 1999, A&A, 342, 717
Bacciotti, F., Mundt, R., Ray, T. P., et al. 2000, ApJ, 537, L49
Bacon, R., Adam, G., Baranne, A., et al. 1995, A&AS, 113, 347
Brugel, E. W., Mundt, R., & Bührke, T. 1984, ApJ, 287, L73
Canto, J., Rodriguez, L. F., Barrall, J. F., & Carrall, P. 1981, ApJ, 244, 102
Close, L. M., Roddier, F., Hora, J. L., et al. 1997, ApJ, 489, 210
Davis, C. J., Berndsen, A., Smith, M. D., Chrysostomou, A., & Hobson, J. 2000, MNRAS, 241
Herbig, G. H. 1968, ApJ, 152, 439
Itoh, Y., Kaifu, N., Hayashi, M., et al. 1999, in Star Formation 1999, ed. T. Nakamoto (Nobeyama Radio Obs.), 304
Jones, B. F., & Herbig, G. H. 1982, AJ, 87, 1223
Greenstein, J. L., Kazarian, M. A., Magakian, T. Yu., & Khachikian, E. Ye. 1976, Afz, 12, 587
Greenstein, J. L., Kazarian, M. A., Magakian, T. Yu., & Khachikian, E. Ye. 1979, Afz, 15, 615
Magakian, T. Yu., & Movsessian, T. A. 1995, A&A, 295, 504
Magakian, T. Yu., & Movsessian, T. A. 1997, in Low Mass Star Formation: From Infall to Outflow, ed. F. Malbet & A. Castets, Poster Proceed. IAU Symp. 182, Grenoble, 158
Movsessian T., & Magakian T. 1999, in Optical and Infrared Spectroscopy of Circumstellar Matter, ed. E. Guenther, B. Stecklum, & S. Klose, ASP Conf. Ser., 188, 49
Raga, A. C. 1986, AJ, 92, 637
Reipurth, B., & Heathcote, S. 1991, A&A, 246, 511
Shibata, K., & Kudoh, T. 1999, in Star Formation 1999, ed. T. Nakamoto (Nobeyama Radio Obs.), 263
Stockton, A., Chesley, D., & Chesley, S. 1975, ApJ, 199, 406
Thé, P. S., de Winter, D., & Pérez, M. R. 1994, A&AS, 104, 315
Walsh, J. R., & Malin, D. F. 1985, MNRAS, 217, 31
Wiseman, J. Wootten, A., Zinnecker, H., & McCaughrean, M. 2001, ApJ, 550, L87